6106 *Macromolecules* **2010**, *43*, 6106–6112
DOI: 10.1021/ma101039y

Macromolecules
ARTICLE

Optically Active Multi-Walled Carbon Nanotubes for Transparent, Conductive Memory-Shape Polyurethane Film

Yong Chae Jung,[†] Hyun Hee Kim,[‡] Yoong Ahm Kim,*[,†] Jin Hee Kim,[†] Jae Whan Cho,*[,‡] Morinobu Endo,[†] and Mildred S. Dresselhaus[§]

[†]*Faculty of Engineering Shinshu University, 4-17-1 Wakasato, Nagano-shi 380-8553, Japan,*
[‡]*Department of Textile Engineering, Konkuk University, Seoul 143-701, Korea, and*
[§]*Massachusetts Institute of Technology Cambridge, Massachusetts 02139-4307*

Received May 12, 2010; Revised Manuscript Received June 16, 2010

ABSTRACT: We have fabricated electrically conductive, optically transparent, and mechanically strong shape-memory polyurethane film by incorporating photochemically surface-modified multiwalled carbon nanotubes (MWNTs). The oxygen functional groups on the sidewall of the MWNTs, created by vacuum ultraviolet light, provide reactive sites to bind strongly with polyurethane. The homogeneous dispersion of MWNTs is confirmed by the optical signals coming from the innermost tube (ca. 0.9 nm) of the MWNTs, not from isolated single walled carbon nanotubes. The optimally introduced functional groups as well as the judicious selection of organic solvent, both for dispersing MWNTs homogeneously and dissolving the polymer completely, are critical to fabricate high functional polyurethane film.

Introduction

Polyurethanes have been widely used in common life as adhesives, coatings, elastomers, and biomedical materials, because they have relatively good biocompatibility and a high resistance to chemicals as well as excellent processability.[1] From the viewpoint of structure, polyurethanes exhibit noticeable phase separations at the microscale arising from hard and soft segments, where the latter are responsible for the evolution of the shape−memory effect.[2−4] In order to use them as smart fabrics (or intelligent textiles) that have the ability of actuation against environmental forces in a controllable manner,[5] single- or multiwalled carbon nanotubes (SWNTs or MWNTs) have been examined as electrically and thermally conducting as well as mechanically reinforcing fillers in polyurethane.[6−15] Ideally, carbon nanotubes have a small diameter and a long length, but should be individually dispersed within a polymer matrix in order to exploit the superior mechanical and electrical properties of nanotubes. However, SWNTs were easily shortened down to 50 nm in the individualization process,[16] and furthermore, SWNTs experienced a depression in their optical activity due to their covalently attached functional groups.[17] On the other hand, it is not easy to evaluate the dispersion state of optically silent large-diameter MWNTs.[18]

Here, we suggest that optically active MWNTs are the best filler for polyurethane, in particular for applications where electricity, optical transparency and mechanical strength are needed simultaneously, due to the following reasons: (1) The length of individually dispersed MWNTs is larger than that of SWNTs because MWNTs are more resistant than SWNTs to the hydrodynamic shear forces generated by the ultrasonication process.[19] (2) Their small diameter (below 10 nm), including a small portion of optically active innermost tubes (ca. 0.9 nm) is beneficial to provide high optical transparency in polyurethane film. (3) Individual MWNTs are known to show a metallic character in their electrical conductance.[20]Finally (4), their expected production cost (ca. $50 US/g) is significantly lower than that of SWNTs. In addition, we have adopted an environmentally friendly vacuum ultraviolet (VUV) treatment as the chemical modification tool for the sidewall of MWNTs,[21] and the use of *N*-methylpyrrolidone (NMP) as both a dispersing agent for MWNTs and a solvent for polyurethane. We have demonstrated that the optical signals arise from the innermost tube of MWNTs, and do not come from isolated SWNTs through a detailed optical study of VUV-treated MWNTs. The purpose of the present study is to examine the dispersion state of MWNTs in polyurethane with the help of optical spectroscopies, and the effect of the incorporation of such MWNTs on the electrical and thermal conductivity, optical transparency, and mechanical properties of MWNT-filled polyurethane film.

Experimental Section

Synthesis and Surface Functionalization of MWNTs. Catalysts for growing carbon nanotubes were prepared by the following procedures. After dissolving a specified amount of $Fe(NO_3)_3 \cdot 9H_2O$ and $(NH_4)_6Mo_7O_2 \cdot 4H_2O$ in ethanol, the mixed Fe−Mo solution was introduced into a suspension of MgO powder, followed by sonication for 1 h. In this experiment, the weight ratio of Fe/Mo/MgO was 1/1/40. After drying, the material was baked in a vacuum at 150 °C for 24 h and then ground with a mortar pestle. The ground catalyst powder was introduced into the center of the reactor. Finally, by passing the mixed gases (argon + methane = 1/1) into the reactor at 875 °C for 15 min, we were able to synthesize MWNTs. To get high purity tubes, we applied a two-step purification process: high-temperature oxidation to remove both chemically active SWNTs and amorphous carbon deposited on the outer-shell of carbon nanotubes (500 °C for 30 min) and hydrochloric acid treatment (100 °C for 8 h) to dissolve the entrapped metallic particles and MgO. In order to introduce oxygen functional groups onto the sidewall of the tubes, a highly purified MWNT sample was exposed to VUV (UER172−200, Ushio Inc.) (λ_{max} = 172 nm) light using a xenon

*Corresponding authors: (Y.A.K.) Telephone: +81-26-269-5212. Fax: +81-26-269-5208. E-mail: yak@endomoribu.shinshu-u.ac.jp. (J.W.C.) Telephone: +82-2-450-3513. Fax: +82-2-457-8895. E-mail: jwcho@konkuk.ac.kr.

 Published on Web 06/30/2010

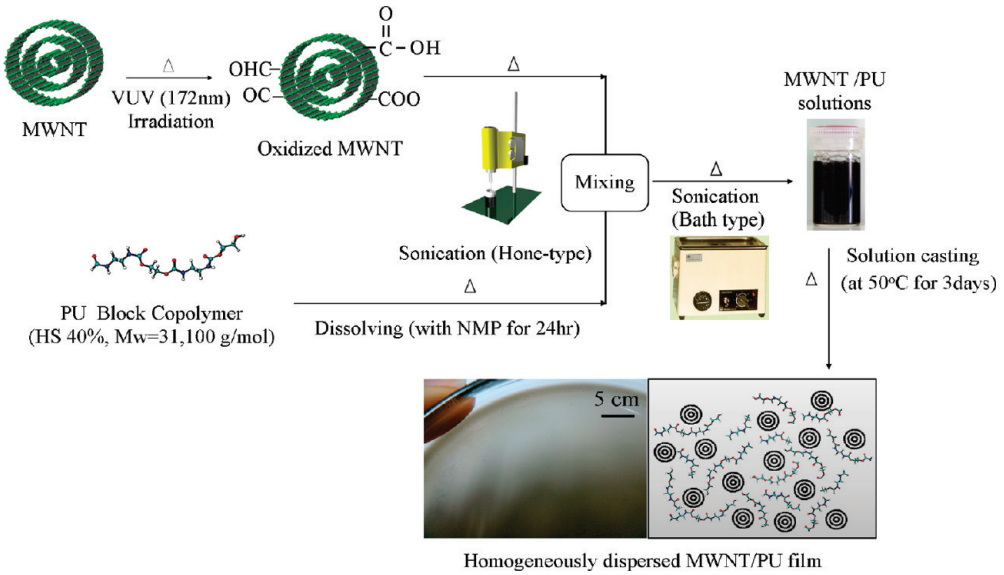

Figure 1. Schematic procedure for fabricating optically active multiwalled carbon nanotube-reinforced shape−memory polyurethane film.

excimer lamp under atmospheric conditions for 1, 10, 30, and 60 min. The power of the irradiated light was limited to 10 W/cm^2 by fixing the distance between the VUV lamp and the sample at 20 mm.

Polymerization of Shape-Memory Polyurethane Block Copolymers. Poly(ε-carprolactone)diol (PCL, Solvay Co., MW = 3000 g/mol), 4,4-methylene bis(phenylisocyanate) (MDI, Junsei Chemical), and 1,4-butandiol (BD, Ducksan Chemical) were used for the synthesis of polyurethane. In a 500 mL four-neck, cylindrical vessel equipped with a mechanical stirrer, calculated amounts of MDI and PCL in 100 mL of freshly distilled dimethylacetamide were stirred under nitrogen at 80 °C for 3 h, to make the prepolymer. Then, BD was added dropwisely to the prepolymer. When the polymerization was over, the polyurethane was removed with the use of a solvent under vacuum, and the resulting material was further solidified by storing it in an oven at 100 °C for 24 h. The precursor for polyurethane with a molar ratio of 6/1/5 of MDI/PCL/BD was used for obtaining a hard segment content of 40 wt %, and an average molecular weight of the synthesized PU was 31 159 g/mol from a GPC measurement.

Fabrication of the MWNT-Reinforced Polyurethane Film. The photochemically treated MWNTs (1 mg) were dispersed in NMP (10 mL) under strong ultrasonication (US-300T, NIHONSEIKI KAISHA Ltd.) for 30 min at 4 °C. Then, the polyurethane (2 g) was completely dissolved in a three-neck flask containing of NMP (20 mL) solvent at room temperature and the mixture was stirred for 1 day. Two prepared solutions were mixed for 1 h and then subjected to a bath-type sonicator (Branson 2510) at 4 °C for 2 h in order to ensure a homogeneous dispersion of the tubes in the polyurethane solution. Finally, the MWNT-filled (0.5 wt %) polyurethane film with a thickness of ca. 0.51 μm was obtained using a solution cast method by removing the residual solvent using a vacuum dryer at 50 °C for 3 days.

Structural Characterizations. Raman, absorption spectra, and photoluminescence maps were obtained using a Kaiser Holo-Lab5000 system (532 and 633 laser lines), a UV−vis−NIR spectrophotometer (Shimadzu soildspec-3700) and a Shimadzu NIR-PL system. The macro-morphology of the photochemically treated MWNTs was observed using field emission scanning microscopy (FE-SEM) (JSM6335Fs), and transmission electron microscopy (TEM) measurements were carried out in order to observe the morphology of the nanotubes by using HRTEM (JEOL2010FEF). We also carried out differential scanning calorimeter measurements (TA Instruments 2010 DSC Dupont) for all samples in order to understand the effect of the reinforced tubes on the thermal stability of polyurethane film (heating rate = 10 °C/min). The electrical conductivity of the obtained film was measured using a LORESTA-GP (Mitsubishi Chemical, MCP-T600) electric analyzer. A standard four probe (TFP type probe) method was used to measure the electrical conductivity for all of the composites films at ambient conditions of 25 °C. The thermal conductivity of a rectangular (1 × 1 cm) shaped film was measured using a steady-state heat flow measurement apparatus (LFA447-Nanoflash, NETZSCH). The mechanical properties of the specimens were evaluated at room temperature according to the ASTM D638 test method using a tensile tester (UTM LR50K; JJ Lloyd, Centre for Materials Research, University of London, London, U.K.) for a dog-bone type dumbbell specimen. The dimensions of the specimens were 60 (length) × 10 (width) × 10 (narrow portion length) × 3 (narrow portion width) × 0.50 (thickness) mm. We have used the following measurement conditions: gauge length = 25 mm; crosshead speed = 10 mm/min; load cell = 2.5 kN. At least three samples were tested and the average of each property measurement was used.

Results and Discussion

Using catalytically grown small-diameter MWNTs that were prepared by a catalytic chemical vapor deposition method and polymerized shape-memory polyurethane block copolymers (see detailed synthetic conditions in the Experimental Section), we have fabricated MWNT-filled polyurethane film according to the following procedures, as described in Figure 1. First, photochemically treated MWNTs, as described below, were dispersed in NMP under strong ultrasonication, whereas the polyurethane was completely dissolved in NMP solvent. Two prepared solutions were subjected to a bath-type sonicator in order to ensure the homogeneous dispersion of the tubes in the polyurethane solution. Finally, a MWNT-filled polyurethane film (with a thickness of ca. 0.51 μm) was obtained using a solution cast method by removing the residual solvent using a vacuum dryer.

According to SEM and TEM observations, the nanotube sample synthesized in our study is severely entangled without any particle-like impurities (see Figure 2a and inset in Figure 2a) in which each MWNT is relatively straight and consists of three to six concentric layers (or tubes with small-sized diameter below 10 nm) (Figure 2e). In order to fully exploit the intrinsic physical properties of nanotubes in a polymer matrix and thus to achieve high-performance polymer composites, intensive and extensive

studies of the homogeneous dispersion of carbon nanotubes have been carried out. Generally, strong acid treatments have been adopted to disentangle the strongly bundled nanotubes as well as to provide a hydrophilic behavior to the sidewall of the tubes.[22−25] Alternatively, we have developed a photochemical method to introduce functional groups on the sidewall of the tubes.[17,21] More specifically, by exposing the as-prepared nanotube sample to vacuum ultraviolet (VUV) light under atmospheric conditions for 1, 10, 30, and 60 min, respectively, we have activated the hydrophobic sidewalls of nanotubes. Then, the morphological changes in both the bundled structure and in the tubular morphology of MWNTs by photochemical treatment are observed. SEM images in Figure 2 (a-d) revealed that there is no apparent change in the bundled features of MWNTs as a function of photochemical treatment time. The pristine MWNTs consist of six concentric shells (diameter = 8 nm) and have a relatively clean (or smooth) outer surface (Figure 2e). However, it is observed that the photochemically treated tubes (Figure 2f−h) exhibited modified structures including a roughened external surface. In other words, the chemically active oxygen species, generated by VUV light, preferentially reacts with the near-surface of the tubes and thus gives rise to a partial structural perturbation at the near-surface of the tubes. For tubes photochemically treated for 10 min (Figure 2b,f), there are no distinctive structural changes nor is there any loss of mass, indicating that photochemical reactions caused by ultraviolet light occur under mild conditions. However, with further longer treatment up to 60 min, the observation of a structural perturbation at the near-surface of the tubes can be explained by the severe oxidative etching of the nanotubes that might induce a substantial degradation of the physical and electrical properties of the tubes.

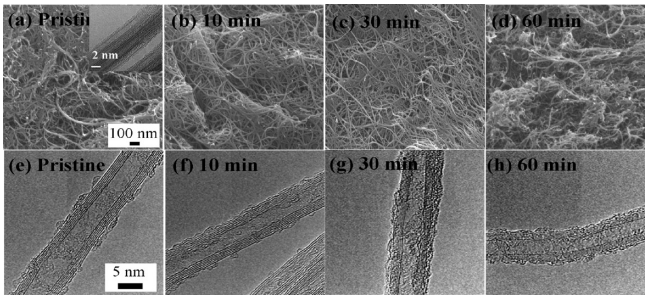

Figure 2. SEM and TEM images of the pristine (a, e) and the tubes that are photochemically treated for 10 min (b, f), 30 min (c, g), and 60 min (d, h), respectively.

In order to evaluate the degree of structural perturbation of the tubes via photochemical treatment, the Raman characterization tool was chosen because of its high sensitivity to the crystallinity of the near surface.[26,27] Raman spectra using 532 nm laser excitation were taken for the pristine and photochemically treated tubes, as shown in Figure 3a. There is a relatively sharp, strong G-band (E_{2g2} graphite mode) around 1585 cm^{-1} and a broad D-band (defect-induced mode) at 1350 cm^{-1}.[28] It is noted that the G-band was continuously suppressed, the D band became linearly intensified and the R value (defined as I_D/I_G, the integrated intensity of the D band divided by the integrated intensity of the G band) is continuously increased, in proportion to the photochemical treatment time. This result suggests that a certain amount of structural disorder was generated by the preferential attack of oxygen species on the sidewall of the tubes. At the same time, oxygen-related functional groups are expected to be introduced on the outer surface of the tubes via such a photochemical treatment. Therefore, C 1s XPS spectra were taken to evaluate the functional groups on the outer surface of the MWNTs that were subjected to photochemical treatment in a semiquantitative way (Figure 3b). The strong peak at 284.3 eV can be assigned to the sp^2-bonded carbon atoms, while the broad peak at 285.2 eV originates from the sp^3-bonded carbon atoms (i.e., dangling bonds).[29,30] Even though there is no apparent change in the C 1s XPS spectra of the tubes by photochemical treatment (Figure 3b), we found that the relative concentration of oxygen atoms is saturated for the tubes that are photochemically treated for 30 min (Table 1). In addition, the intensified peaks of −COOH, −COO, and −C−O− at 290.5, 288.6, and 286.7 eV also indicate a substantial introduction of oxygen-containing functional groups on the outer surface of the tubes.

Among a variety of organic solvents, NMP is judiciously selected in our study because of its dual ability to solubilize polyurethane as well as to disperse the strongly bundled nanotubes.[31−33] Thus, we have examined the effect of the oxygen functional groups of the sidewall of the tubes on the dispersibility (or solubility) of photochemically treated tubes in NMP. More specifically, 1 mg of tubes was dispersed in NMP (10 mL) under sonication (KUBOTA UP50H) for 1 h at 5 °C. Subsequently, these nanotube suspensions (containing carbon nanotubes) were subjected to an ultracentrifuge (20,000 g) for 1 h in order to remove the insoluble materials. All nanotube suspensions are opaque (see inset in Figure 4a), making it difficult to distinguish the dispersibility of tubes with the naked eye. Therefore, UV-absorption spectra were taken from all nanotube suspensions in order to look for a subtle difference in the dispersibility of the tubes due to their environment. All nanotube suspensions showed

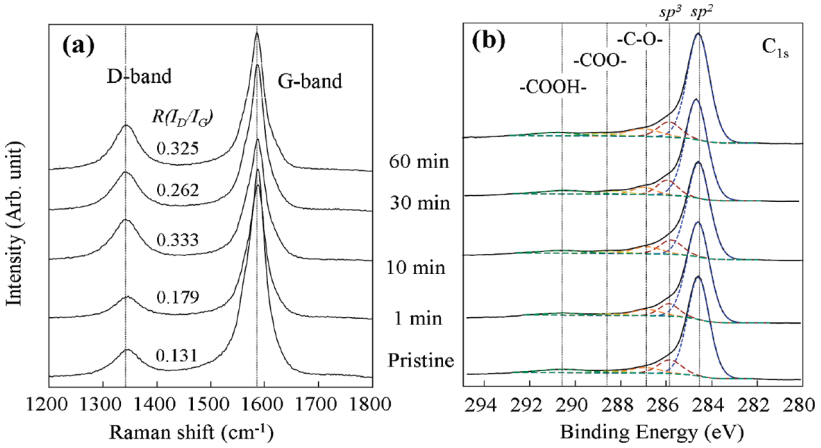

Figure 3. (a) Raman spectra and the C 1s XPS spectra of the pristine and the photochemically treated MWNTs for irradiation times ranging from 1 to 60 min.

Table 1. Relative Atomic Concentration of Carbon and Oxygen for the Pristine and the Photochemically Oxidized MWNTs, Respectively

samples codes	−C−O− (%)	−COO− (%)	−COOH− (%)	carbon (%)	oxygen (%)	O/C	sp^2/sp^3 [a]
pristine	5.7	1.8	5.4	98.5	1.4	0.015	6.478
irradiation for 1 min	6.2	1.3	2.3	97.6	2.4	0.024	8.943
irradiation for 10 min	6.9	2.5	4.0	96.1	3.9	0.040	6.577
irradiation for 30 min	5.6	3.1	5.5	96.0	4.0	0.041	7.118
irradiation for 60 min	7.6	2.7	4.1	95.5	4.1	0.047	7.009

[a] sp^2/sp^3 is the integrated intensity of the sp^2-carbon assigned peak at 285.2 eV divided by the integrated intensity of the sp^3-carbon assigned peak at 284.3 eV.

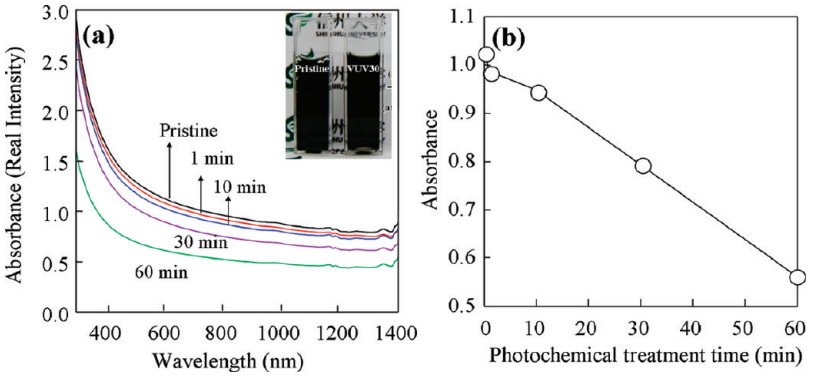

Figure 4. (a) Optical absorption spectra of the pristine and the photochemically treated MWNT suspensions, and (b) variation of the measured absorbance at 700 nm for tubes that are photochemically treated for irradiation times ranging from 1 to 60 min. The photo (inset in part a) shows opaque nanotubes suspensions, indicating that the pristine tubes and tubes photochemically treated for 30 min are homogeneously dispersed in NMP.

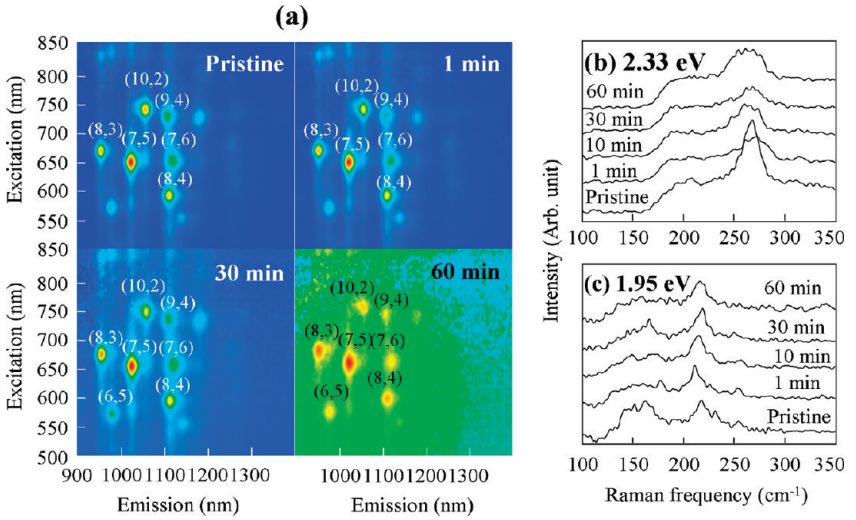

Figure 5. (a) Photoluminescence maps and low-frequency Raman spectra using a laser excitation energy of 2.33 eV (b) and 1.95 eV (c) for the pristine tubes and for the photochemically treated tubes using irradiation times ranging from 1 to 60 min.

similar absorption profiles to conventional carbon materials (Figure 4a). Since the real intensity of the absorbance is directly proportional to the amount of dispersed nanotubes within the solution,[33−36] the linearly decreased absorbance at a wavelength of 700 nm as a function of photochemical treatment time (Figure 4b) indicates that the oxygen functional groups are detrimental to the solubility of the nanotubes in NMP. However, when looking at the absorption profiles very carefully, we are able to see small but clear absorption peaks around 1000, 1200, and 1350 nm that are expected to be related to Van Hove singularities (VHS). Noticeably, with longer photochemical treatment, there is no apparent change in shape and position of the absorption peaks and this suggests that these absorption peaks are coming from the semiconducting innermost tubes of the MWNTs, and not from isolated SWNTs. Very recently, we have demonstrated that only 10 min of photochemically treatment of SWNTs is sufficient to show a severely quenched luminescence peak and the weak, broad absorption peaks that are observed.[17] Such a breakdown of the VHS was identified by the substantial decoration of the functional groups on the sidewall of the SWNTs.

Furthermore, in order to obtain additional experimental evidence for the presence of VHS from the innermost tube of MWNTs, and not from isolated SWNTs, we measured the photoluminescence (PL) map (Figure 5a) and low frequency Raman spectra (Figure 5b,c) for all the nanotube suspensions. The pristine MWNT solutions exhibited strong PL peaks, which are assigned to the innermost semiconducting tubes of the MWNTs with chiralities of (10, 2), (8, 3), (7, 5), and (8, 4). Noticeably, no change in the position and intensity of the PL peaks were observed for the MWNTs that were photochemically treated for 30 min, indicating that outer multishells effectively protected the innermost tubes against oxidation. With further photochemical treatment up to 60 min, we still observed the PL peaks. In addition, we have clearly observed the radial breathing

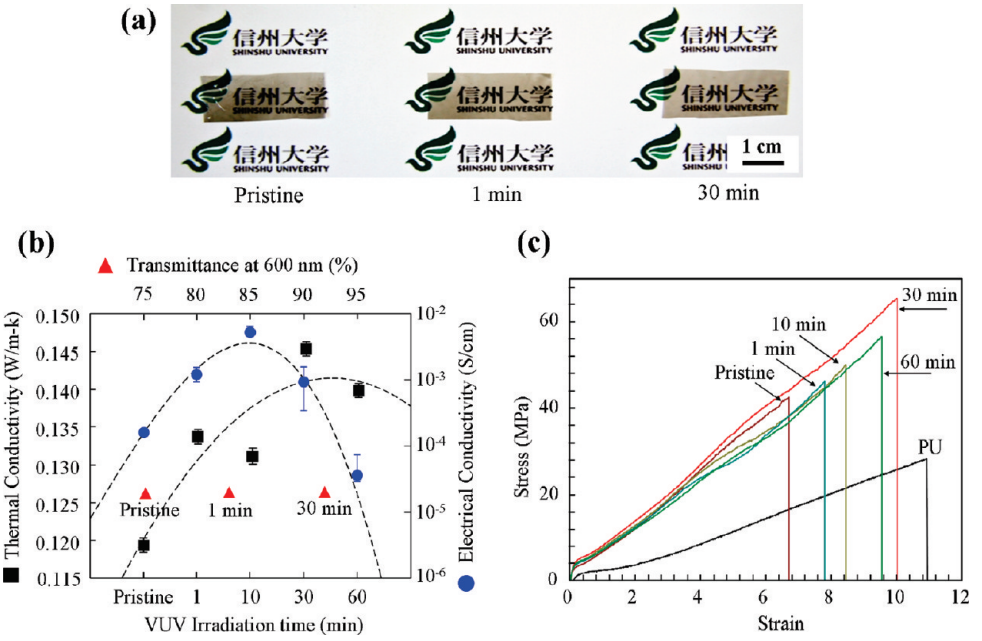

Figure 6. (a) Semitransparent MWNT-filled polyurethane films using the pristine tubes and the tubes photochemically treated for 1 and 30 min. (b) Variations of the optical transmittance, thermal conductivity and electrical conductivity of MWNT-filled polyurethane films when incorporating the pristine and the photochemically treated tubes for irradiation times ranging from 1 to 60 min. (c) Stress−strain curves of pure polyurethane and MWNT-filled polyurethane films. Note that the addition of the photochemically treated tubes for 30 min allows polyurethane to have a high optical transparency, a good thermal and electrical conductivity as well as a highly enhanced tensile property.

Table 2. Mechanical Properties of the Pure and MWNTs-Filled Polyurethane Block Copolymer Films

sample ID		modulus (MPa)	tensile strength (MPa)	elongation-at-break (%)
pure polyurethane		4.5	33.5	1092
polyurethane composite films by incorporating	pristine	32.9	42.8	671
0.5 wt % of VUV-treated MWNTs	1 min	37.6	46.3	782
	10 min	39.8	50.6	843
	30 min	42.5	65.1	1010
	60 min	32.8	57.2	958

mode peaks at 260 cm^{-1} (Figure 5b) and 220 cm^{-1} (Figure 5c) from the MWNTs that were photochemically treated up to 60 min. From those optical studies, we are able to conclude that the strong optical signals are coming from the innermost tube of the MWNTs, and not from isolated SWNTs. Even though we have confirmed the presence of VHS in our MWNT sample, further optical studies in detail have to be carried out in order to understand the effect of intershell interactions on the optical properties of MWNTs.

Regarding MWNTs-reinforced (ca. 0.5 wt %) polyurethane composites in the form of a film (ca. 0.51 μm thick), we have carried out a systematic analysis in order to understand the influence of photochemically introduced functional moieties as well as the degree of dispersion of the MWNTs on the optical and physical properties of polyurethane films. All films that are prepared via solution casting are semitransparent, and thus we are not able to see the difference in visual appearance of the films when measuring the parameter of the photochemical treatment time with the naked eye (Figure 6a). However, we found that the optical transmittance of a MWNT-filled polyurethane film relative to a pure (unfilled) polyurethane film increased from 75 to 94% when adding MWNTs that are photochemically treated for 30 min (Figure 6b). This optical study proved that tubes that are photochemically treated for 30 min have the optimized amount of oxygen-containing functional groups (or hydrophilic nature) and thus exhibited the best dispersibility within the polyurethane polymer. Concurrently, we observed a maximum value in both the thermal conductivity (0.146 W/(m k)) and the electrical conductivity (1.58×10^{-3} S/cm) of MWNTs-filled polyurethane film when tubes that are photochemically treated for 10 and 30 min are incorporated within the polyurethane film (Figure 6b). These enhancements in the thermal conductivity and the electrical conductivity in MWNT-filled polyurethane film can be explained by the increased density of photochemically generated active sites that have the ability to bind with the polyurethane polymer at the molecular level, and thus are beneficial for the homogeneous dispersion of the tubes within a polymer matrix (the early formation of a percolation threshold) as well as to reduce the interfacial phonon scattering.[37] When adding tubes that are photochemically treated for 60 min, the decreased value in the thermal conductivity and electrical conductivity of the polyurethane film is a result of the deteriorated physical properties of the tubes caused by the severe oxidative etching process. In addition, the effect of the photochemically introduced functional groups is clearly verified in the largely improved mechanical properties of MWNTs-filled polyurethane film. Figure 6c shows the stress−strain curves, indicating that the addition of MWNTs surely improves the tensile properties of film. These mechanical properties, such as the modulus, tensile strength and elongation-at-break are summarized in Table 2. Noticeably, the addition of the tubes that are photochemically treated for 30 min allows the polyurethane film to have a 10 times enhanced modulus and a two-times enhanced tensile strength, without any loss of their elongation-at-break, compared to the corresponding values of the pure polyurethane film. Conclusively, the optimally introduced carboxyl groups on the hydrophobic sidewall of the tubes without any deterioration of their physical properties by the photochemical treatment were essential for improving the interaction

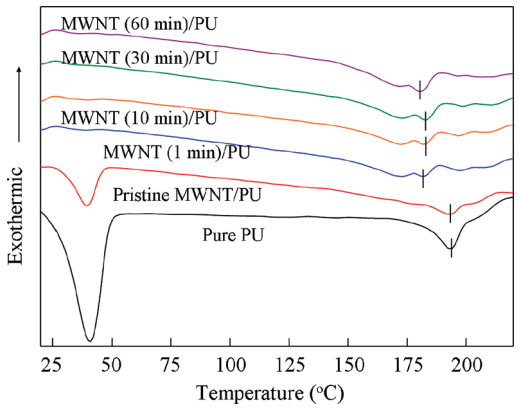

Figure 7. Differential scanning calorimetry curves of the pure polyurethane and MWNT-filled polyurethane films in which nanotubes are photochemically treated for irradiation times from 1 to 60 min.

Table 3. Thermal Properties of the Pure and MWNTs-Filled Polyurethane Block Copolymer Films

	Soft segment		Hard segment	
samples	T_m (°C)[a]	H_m (J/g)[b]	T_m (°C)[c]	H_m (J/g)[d]
pure PU	40.6	16.55	193.5	2.62
pristine MWNT/PU	39.1	5.31	192.7	1.13
MWNT (1 min)/PU	38.7	0.14	182.2	0.32
MWNT (10 min)/PU	39.4	0.09	182.8	0.35
MWNT (30 min)/PU	32.1	0.06	183.4	0.51
MWNT (60 min)/PU	35.6	0.12	180.9	0.79

[a] T_m means melting temperature of soft segment. [b] H_m means heat of fusion of soft segment. [c] T_m means melting temperature of hard segment. [d] H_m means heat of fusion of hard segment.

with the OH groups in the polyurethane chain or the $\pi-\pi$ interaction strength between the tubes and polyurethane, and thus to improve the thermal, electrical and physical properties of the polyurethane film.

Finally, in order to determine in detail the effect of the addition of MWNTs on the thermal properties of the polyurethane, we have carried out differential scanning calorimeter measurements (Figure 7, Figure S1, and Table 3). The pure polyurethane polymer exhibited a sharp endothermic peak around 40 °C (which is assigned to the melting of the soft segment) and also exhibited a small but broad peak at 193 °C (which could be assigned to the melting of the hard segment).[1] With increasing photochemical treatment time up to 30 min, for both the soft and hard segments, we observed that the melting temperature decreased and the heat of fusion decreased abruptly. However, the drastic change in the soft segment domain suggests that nanotubes affect the change in the morphology of the polyurethane composites. In addition, we have confirmed the improved thermal stability of polyurethane film by the presence of MWNTs (Figure S1).

Conclusions

We fabricated optically transparent, mechanically strong, and electrically and thermally conductive shape-memory polyurethane block copolymer films by incorporating a small amount of the homogeneously dispersed but optically active MWNTs (ca. 0.5 wt %). The effectiveness of the photochemical treatment as a sidewall functionalization tool for MWNTs was demonstrated by the 10 times increased modulus as well as by the doubled tensile strength without any loss of elongation-at-break. We also have demonstrated the optical signals arising from the innermost tube of the MWNTs and not from isolated SWNTs through a detailed optical study of photochemically treated MWNTs. We believe that MWNT-filled multifunctional shape-memory polyurethane block copolymer films will find their end usage in smart fabrics (or intelligent textiles) in the future.

Acknowledgment. We acknowledge the support from the Regional Innovation Cluster Program of Nagano and a Grant-in-Aid (Nos. 19002007, and 20510096) from the Ministry of Education, Culture, Sports, Science and Technology of Japan. This research was supported by Basic Science Research Program through the National Research Foundation of Korea (NRF) funded by the Ministry of Education, Science and Technology of Korea (R11-2005-065). J.H.K. acknowledges the support of Shinshu University Global COE Program "International Center of Excellence on Fiber Engineering". M.S.D. acknowledges support from US NSF Grant DMR-07-04197.

Supporting Information Available: TGA thermograms of the pure polyurethane and MWNT-filled polyurethane nanocomposites films (Figure S1). This material is available free of charge via the Internet at http://pubs.acs.org.

References and Notes

(1) Hepburn, C. *Polyurethane Elastomers*; Elsevier Applied Science: New York, 1993.
(2) Liang, C.; Rogers, C. A.; Malafeew, E. *J. Intell. Mater. Struct.* **1997**, *8*, 380–386.
(3) Richard, F.; Gordon, P. E. *Mater. Technol.* **1993**, *8*, 254–258.
(4) Lee, B. S.; Chun, B. C.; Chung, Y.-C.; Sul, K. I.; Cho, J. W. *Macromolecules* **2001**, *34*, 6431–6437.
(5) Tao, X. *Smart Fibres, Fabrics and Clothing: Fundamentals and Applications*; Woodhead Publishing Ltd.: Cambridge, U.K., 2001.
(6) Koerner, H.; Price, G.; Pearce, A.; Alexander, M.; Vaia, R. V. *Nat. Mater.* **2004**, *3*, 115–120.
(7) Sen, R.; Zhao, B.; Perea, D.; Itkis, M. E.; Hu, H.; Love, J.; Bekyarova, E.; Haddon, R. C. *Nano Lett.* **2004**, *4*, 459–464.
(8) Kuan, H. C.; Ma, C. C. M.; Chang, W. P.; Yuen, S. M.; Wu, H. H.; Lee, T. M. *Compos. Sci. Technol.* **2005**, *65*, 1703–1710.
(9) Kwon, J. Y.; Kim, H. D. *J. Polym. Sci., Part A: Polym. Chem.* **2005**, *43*, 3973–3985.
(10) Cho, J. W.; Kim, J. W.; Jung, Y. C.; Goo, N. S. *Macromol. Rapid Commun.* **2005**, *26*, 412–416.
(11) Jung, Y. C.; Sahoo, N. G.; Cho, J. W. *Macromol. Rapid Commun.* **2006**, *27*, 126–131.
(12) Xiong, J.; Zhou, D.; Zheng, Z.; Yang, X.; Wang, X. *Polymer* **2006**, *47*, 1763–1766.
(13) Ryszkowska, J.; Jurczyk-Kowalska, M.; Szymborski, T.; Kurzdlowski, K. J. *Physica E* **2007**, *39*, 124–127.
(14) Buffa, F.; Abraham, G. A.; Grady, B. P.; Resasco, D. *J. Polym. Sci., Part B: Polym. Phys.* **2007**, *45*, 490–501.
(15) Chen, X.; Wang, J.; Zou, J.; Wu, X.; Chen, X.; Xue, F. *J. Appl. Polym. Sci.* **2009**, *114*, 3407–3413.
(16) Sun, X.; Zaric, S.; Daranciang, D.; Welsher, K.; Lu, Y.; Li, X.; Dai, H. *J. Am. Chem. Soc.* **2008**, *130*, 6551–6555.
(17) Lee, S. H.; Jung, Y. C.; Kim, Y. A.; Muramatsu, H.; Teshima, K.; Oishi, S.; Endo, M. *Nanotechnology* **2009**, *20*, 105708–5.
(18) Dresselhaus, M. S.; Dresselhaus, G.; Saito, R.; Jorio, A. *Phys. Rep.* **2005**, *409*, 47–99.
(19) Green, A. A.; Hersam, M. C. *Nature Nanotechnol.* **2009**, *4*, 64–70.
(20) Bachtold, A.; Strunk, C.; Salvetat, J.-P.; Bonard, J.-M.; Forró, L.; Nussbaumer, T.; Schönenberger, C. *Nature* **1999**, *397*, 673–675.
(21) Lee, S. H.; Teshima, K.; Jang, I. Y.; Yubuta, K.; Kim, Y. J.; Kim, Y. A.; Shishido, T.; Endo, M.; Oishi, S. *Chem. Commun.* **2010**, *46*, 2295–2297.
(22) Mawhinney, D. B.; Naumenko, V.; Kuzenetsova, A.; Yates, J. T. J.; Liu, J.; Smalley, R. E. *J. Am. Soc.* **2000**, *122*, 2382–2384.
(23) Nagasawa, S.; Yudasaka, M.; Hirahara, K.; Ichihashi, T.; Iijima, S. *Chem. Phys. Lett.* **2000**, *328*, 374–380.
(24) Hu, H.; Zhao, B.; Itkis, M. E.; Haddon, R. C. *J. Phys. Chem. B* **2003**, *107*, 13838–13842.
(25) Zhang, J.; Zou, H.; Qing, Q.; Yang, Y.; Li, Q.; Liu, Z.; Guo, X.; Du, Z. *J. Phys. Chem. B* **2003**, *107*, 3712–3718.
(26) Pimenta, M. A.; Dresselhaus, G.; Dresselhaus, M. S.; Cancado, L. G.; Jorio, A.; Saito, R. *Phys. Chem. Chem. Phys.* **2007**, *9*, 1276–1291.

(27) Cancado, L. G.; Takai, K.; Enoki, T.; Endo, M.; Kim, Y. A.; Mizusaki, H.; Coelho, L. N.; Magalhaes Paniago, R.; Jorio, A.; Pimenta, M. A. *Appl. Phys. Lett.* **2006**, *88*, 163106–3.
(28) Dresselhaus, M. S.; Eklund, P. C. *Adv. Phys.* **2000**, *49*, 705–814.
(29) Ago, H.; Kugler, T.; Cacialli, F.; Salaneck, W. R.; Shaffer, M. S. P.; Windle, A. H.; Friend, R. H. *J. Phys. Chem. B* **1999**, *103*, 8116–8121.
(30) Murphy, H.; Papakonstantinou, P.; Okpalugo, T. I. T. *J. Vac. Sci. Technol. B* **2006**, *24*, 715–720.
(31) Ausman, K. D.; Piner, R.; Lourie, O.; Ruoff, R. S.; Korobov, M. *J. Phys. Chem. B* **2000**, *104*, 8911–8915.
(32) Giordani, S.; Bergin, S. D.; Nicolosi, V.; Lebedkin, S.; Kappes, M. M.; Blau, W. J.; Coleman, J. N. *J. Phys. Chem. B* **2006**, *110*, 15708–15718.
(33) Bahr, J. L.; Mickelson, E. T.; Bronikowski, M. J.; Smalley, R. E.; Tour, J. M. *Chem. Commun.* **2001**, 193–194.
(34) Qin, Y.; Liu, L.; Shi, J.; Wu, W.; Zhang, J.; Guo, Z.-X.; Li, Y.; Zhu, D. *Chem. Mater.* **2003**, *15*, 3256–3260.
(35) Marsh, D. H.; Rance, G. A.; Zaka, M. H.; Whitby, R. J.; Khlobystov, A. N. *Phys. Chem. Chem. Phys.* **2007**, *9*, 5490–5496.
(36) Hernandez, Y.; Nicolosi, V.; Lotya, M.; Blighe, F. M.; Sun, Z.; De, S.; McGovern, I. T.; Holland, B.; Byrne, M.; Gun'Ko, Y. K.; Boland, J. J.; Niraj, P.; Duesberg, G.; Krishnamurthy, S.; Goodhue, R.; Hutchison, J.; Scardaci, V.; Ferrari, A. C.; Coleman, J. N. *Nature Nanotechnol.* **2008**, *3*, 563–568.
(37) Biercuk, M. J.; Llaguno, M. C.; Radosavljevic, M.; Hyun, J. K.; Johnson, A. T.; Fisher, J. E. *Appl. Phys. Lett.* **2002**, *80*, 2767–2769.